VACUUM ENERGY FOR STATIC, CYLINDRICALLY SYMMETRIC SYSTEMS

An Honors Fellow Thesis

by

CYNTHIA TRENDAFILOVA

Submitted to Honors and Undergraduate Research
Texas A&M University
in partial fulfillment of the requirements for the designation as

HONORS UNDERGRADUATE RESEARCH FELLOW

May 2012

Majors: Mathematics
Physics

VACUUM ENERGY FOR STATIC, CYLINDRICALLY SYMMETRIC SYSTEMS

An Honors Fellow Thesis

by

CYNTHIA TRENDAFILOVA

Submitted to Honors and Undergraduate Research
Texas A&M University
in partial fulfillment of the requirements for the designation as

HONORS UNDERGRADUATE RESEARCH FELLOW

Approved by:

Research Advisor: Stephen Fulling
Associate Director, Honors and Undergraduate Research: Duncan Mackenzie

May 2012

Majors: Mathematics
Physics

ABSTRACT

Vacuum Energy for Static, Cylindrically Symmetric Systems. (May 2012)

Cynthia Trendafilova
Department of Mathematics
Department of Physics
Texas A&M University

Research Advisor: Dr. Stephen Fulling
Department of Mathematics

In my previous thesis for the Undergraduate Research Scholars program I have calculated, both in terms of the scalar field and in terms of the cylinder kernel, the components of the stress-energy tensor of a quantized scalar field for a static, cylindrically symmetric system in the case of locally flat space. I then took these components and expressed them in terms of the known cylinder kernel in cylindrical coordinates. Using these results, I examine the vacuum energy density and pressure in some detail for several different cylindrically symmetric space-times. Results are presented for point-splitting along the t direction, and also for point-splitting along z. Geometries studied include flat space, a cone with various deficit angles, an infinite wedge, and the infinite-sheeted Sommerfeld-Dowker manifold. For all of these cases, the energy density and three pressure components are given for $\xi = \frac{1}{4}$ coupling, and the correction terms for other values of ξ are given as well.

DEDICATION

To my father

ACKNOWLEDGMENTS

I thank my faculty advisor, Dr. Stephen Fulling, for all of his help and guidance throughout the research and writing processes. I thank Mai Truong for her previous work on calculating the cylinder kernel, and I thank Jef Wagner for developing many of the Mathematica strategies used in my calculations.

I am grateful to my family, friends, and research group for all of their support.

This work was supported by NSF Grants No. PHY-0554849 and PHY-0968269.

TABLE OF CONTENTS

Page

ABSTRACT iii

DEDICATION iv

ACKNOWLEDGMENTS v

TABLE OF CONTENTS vi

LIST OF FIGURES vii

CHAPTER

I INTRODUCTION 1

II FLAT SPACE, DOWKER SPACE, AND CONES 6

III WEDGES 15

IV POINT-SPLITTING ALONG Z 20

V CONCLUSION 25

REFERENCES 26

APPENDIX A 28

CONTACT INFORMATION 29

LIST OF FIGURES

FIGURE Page

1 Energy density and pressure as a function of r/t in the Dowker spacetime. 9

2 Energy density and pressure as a function of r/t in the cone spacetime, with $\theta_1 = \pi/4$, 1, and $\pi/2$ (blue, red, yellow). 10

3 Energy density and pressure as a function of θ_1 in the cone spacetime, with $r = 1$. 11

4 Energy density and pressure correction terms as a function of r/t in the Dowker spacetime, with $\beta = 1$. 12

5 Energy density and pressure correction terms as a function of r/t in the cone spacetime, with $\theta_1 = \pi/4$, 1, and $\pi/2$ (blue, red, yellow). 13

6 Energy density and pressure correction terms as a function of θ_1 in the cone spacetime, with $r = 1$ (the concavities visible in (a) and (d) are presumably numerical artifacts). 14

7 Energy density and pressure as a function of r/t in a wedge of angle $\pi/2$, for $\theta = \pi/8$ (blue) and $\theta = \pi/4$ (red). 16

8 Energy density and pressure as a function of θ in a wedge of angle $\pi/2$, for $r = 2$ (blue), $r = 4$ (red), and $r = 8$ (yellow). 17

9 Energy density and pressure corrections as a function of r/t in a wedge of angle $\pi/2$, for $\theta = \pi/8$ (blue) and $\theta = \pi/4$ (red). 18

10 Energy density and pressure corrections as a function of θ in a wedge of angle $\pi/2$, for $r = 2$ (blue), $r = 4$ (red), and $r = 8$ (yellow). 19

11 Energy density and axial pressure as a function of r/z in the Dowker spacetime. 22

12 Energy density and axial pressure as a function of r/z in the cone spacetime, with $\theta_1 = \pi/4$, 1, and $\pi/2$ (blue, red, yellow). 22

FIGURE Page

13 Energy density and axial pressure as a function of θ_1 in the cone spacetime, with $r = 1$. 23

14 Energy density and axial pressure as a function of r/z in a wedge of angle $\pi/2$, for $\theta = \pi/8$ (blue) and $\theta = \pi/4$ (red). 23

15 Energy density and axial pressure as a function of θ in a wedge of angle $\pi/2$, for $r = 2$ (blue), $r = 4$ (red), and $r = 8$ (yellow). 24

CHAPTER I

INTRODUCTION

Within the field of physics, the theory of quantum mechanics, developed in the 1920s, describes the behavior of matter at very small scales. Although we have some physical intuition based on our interactions with the world on a daily basis, the behavior of matter at the smallest scales is much different. Quantum mechanics states that certain physical quantities are quantized and can only occur in discrete amounts rather than a continuous spectrum. Although useful, the theory lacked the scope to describe certain phenomena such as relativistic situations and production and annihilation of particles. By extending it to describe fields, rather than fixed numbers of particles, and taking the fields as the basic physical objects instead, quantum field theory was developed, allowing such issues to be addressed [1, p.48].

By applying quantum field theory, one discovers that vacuum itself usually has a nonzero vacuum energy even where there is no matter present [1, p.96]. This vacuum energy can be calculated for various geometries, and it has been done previously for the cases of flat plates and spherical geometries [2]. Work has also been done to find the pressure on a spherical boundary [2]. Schwartz-Perlov and Olum have calculated the components of the stress-energy tensor previously for the case of a static, spherically symmetric system [3], and the pressure on a boundary has been calculated previously for the spherical case as well [2]. This has also been done for flat, perfectly reflecting boundaries, but it becomes more complicated when the boundaries become curved, because the simple method of images no longer applies; however, there are several methods that can be used [4].

This thesis follows the style of the *European Journal of Physics*.

Other previous work in the field includes Lukosz's work to find the change in the electromagnetic zero-point energy of vacuum in the presence of perfectly conducting surfaces in situations where the problems can be solved by the method of images, such as an infinite wedge of arbitrary angle and a rectangular cavity [5]. Work has also been done by Dowker regarding Green functions for cones and wedges [6] and the Casimir effect in space-times possessing a conical singularity [7]. There has been interest in studying the properties of cylindrical space-times due to their relevance to cosmic strings, which are thin cylinders surrounded by vacuum and usually filled with a non-Abelian gauge field, since the space outside of such strings is described by a cone [8].

However, in spite of this progress in calculating vacuum energy in a variety of cases, there are still problems with the theory which are not fully understood, such as those regarding the energy-balance equation,

$$\frac{\partial E}{\partial h} = -\int_S p_h, \tag{1.1}$$

where h is a general parameter, p_h is the pressure along h, and S is the area of interest. In the cutoff theory used to calculate the energy, this equation is violated [2]. Perhaps examining some properties of cylindrical geometry, which exhibits translational symmetry along an axis and also rotational symmetry around said axis, may provide additional insight into these current paradoxes. While most previous work has examined only total energy, we will also look at energy density and pressure to hopefully provide a better physical interpretation.

In my previous thesis for the Undergraduate Research Scholars program, I focused on vacuum and non-vacuum cylindrically symmetric solutions of Einstein's field equations in

general relativity. I also calculated, both in terms of the scalar field and in terms of the cylinder kernel, the components of the stress-energy tensor of a quantized scalar field for a static, cylindrically symmetric system in the case of locally flat space, using a method analogous to the one utilized by Schwartz-Perlov and Olum [3]. One can make use of the stress-energy tensor formula given in their paper,

$$T_{\mu\nu} = \partial_\mu\phi\partial_\nu\phi - \frac{1}{2}\eta_{\mu\nu}\partial^\lambda\phi\partial_\lambda\phi + \xi[\eta_{\mu\nu}\partial_\lambda\partial^\lambda(\phi^2) - \partial_\mu\partial_\nu(\phi^2)], \tag{1.2}$$

where ϕ is a massless real scalar field satisfying $\ddot{\phi} = \nabla^2\phi$ and ξ is the curvature coupling parameter [3]. They first calculate the components of the stress-energy tensor on the x-axis and then generalize this result to radial and tangential pressures; I used a similar procedure for the case of cylindrical symmetry [3]. I then took these components and expressed them in terms of the known cylinder kernel in cylindrical coordinates. My resulting formulas were

$$T_{00} = \rho = -\frac{1}{2}\partial_t^2\overline{T} + \beta[\partial_r\partial_{r'}\overline{T} + \partial_r^2\overline{T} + \frac{1}{r}\partial_r\overline{T}] \tag{1.3}$$

$$T_{rr} = p_r = -\frac{1}{4}[\partial_r\partial_{r'}\overline{T} - \partial_r^2\overline{T}] - \frac{1}{r}\beta\partial_r\overline{T} \tag{1.4}$$

$$T_{\perp\perp} = p_\theta = \frac{1}{4r}\partial_r\overline{T} + \frac{1}{2r^2}\partial_\theta^2\overline{T} - \beta[\partial_r\partial_{r'}\overline{T} + \partial_r\overline{T}] \tag{1.5}$$

$$T_{zz} = p_z = \frac{1}{2}\partial_z^2\overline{T} - \beta[\partial_r\partial_{r'}\overline{T} + \partial_r^2\overline{T} + \frac{1}{r}\partial_r\overline{T}], \tag{1.6}$$

where $\beta = \xi - \frac{1}{4}$. All off diagonal terms are zero. When I performed these calculations, however, I assumed that the geometry was such that the expectation value of ϕ^2 does not depend on θ. This need not always be the case, and there will be some situations examined in this thesis in which this is not true. In the more general case when ϕ^2 may depend on θ, there is an extra term in the expression for $T_{\perp\perp}$ which does not vanish, and the end result

is that $T_{\perp\perp}$ becomes

$$T_{\perp\perp} = \frac{1}{4r}\partial_r \overline{T} + \frac{1}{4r^2}[\partial_\theta{}^2 \overline{T} - \partial_\theta \partial_{\theta'} \overline{T}] - \beta[\partial_r \partial_{r'} \overline{T} + \partial_r \overline{T}]. \tag{1.7}$$

The cylinder kernel has been found previously by Smith [9] and has also been calculated by Mai Truong [10], in agreement with [9], [11], [12], and [5]. The result in our notation is, for 4-dimensional spacetime,

$$\overline{T}(t,r,\theta,z,r',\theta',z') = -\frac{1}{2\pi\theta_1 rr' \sinh(u)} \frac{\sinh(\frac{2\pi}{\theta_1}u)}{\cosh(\frac{2\pi}{\theta_1}u) - \cos(\frac{2\pi}{\theta_1}(\theta-\theta'))}, \tag{1.8}$$

with u given by $\cosh u = \frac{r^2+r'^2+z^2+t^2}{2rr'}$ [10]. This, along with the components of the stress-energy tensor, can be used to find the vacuum energy and pressure for various cylindrical systems.

There are several configurations for which we examine the vacuum energy density and pressure in some detail. In general, a cylindrically symmetric system has axial symmetry (metric components are independent of the angular coordinate ϕ) and translational symmetry along z (components are also independent of z). One situation we consider is that of a cone, which is described by the metric

$$ds^2 = -dt^2 + dr^2 + r^2 d\phi^2 + dz^2. \tag{1.9}$$

This represents flat space missing a wedge of deficit angle $\Delta\phi = 2\pi - \phi_*$, where ϕ_* is the range of the periodic coordinate ϕ and not necessarily equal to 2π. If $\phi_* > 2\pi$, a wedge is added. Ordinary Minkowski space occurs when $\phi_* = 2\pi$, and this is studied as well as the cone configuration. We also examine the infinite wedge geometry, and the infinite-sheeted Sommerfeld-Dowker manifold given by $\phi_* \to \infty$ and whose Green's function is given in [11].

For all of these cases, the energy density and three pressure components are given for $\xi = \frac{1}{4}$ coupling, and the correction terms for other values of ξ are given as well.

CHAPTER II

FLAT SPACE, DOWKER SPACE, AND CONES

In order to proceed with vacuum energy calculations, there are several tools we need. The first is the components of the stress-energy-momentum tensor, $T_{\mu\nu}$, which describe the energy density and pressure components within a region of space. In the case when the space-time of interest is cylindrically symmetric, static, and locally flat, these components have been calculated in my previous thesis [13]. They are given here in the introduction, with the appropriate generalization made to when the expectation value of ϕ^2 may depend on the θ coordinate. They are presented in terms of the cylinder kernel, $\overline{T}$, which is given by $\frac{\partial \overline{T}}{\partial t} = T$, where $x = (r, \theta, z)$ and $x' = (r', \theta', z')$ are two different points in space. T is defined by $\frac{\partial^2 T}{\partial t^2} = -\nabla^2 T$ with appropriate boundary conditions, the initial condition $T(0, x, x') = \delta(x - x') = \frac{\partial \overline{T}}{\partial t}(0, x, x')$, and a requirement that $T(t, x, x')$ is bounded as $t \to +\infty$ [14]. In the notation used above, the "$\perp$" component has been defined to be along the θ direction, but with respect to an orthonormal basis, so that it has the same physical units as the other components. The parameter $\beta = \xi - 1/4$ is the curvature-coupling parameter, which we initially take to be $\beta = 0$ for simplicity. However, we also examine the correction terms for $\beta \neq 0$ as well.

As mentioned in the introduction, the cylinder kernel has been calculated before, and is given in equation (1.8). The parameter θ_1 describes the periodicity of the θ coordinate in the space-time of interest. Without loss of generality, we have set t' and z' equal to 0, but if we require derivatives with respect to these primed coordinates, we need only replace z by $z - z'$, etc. We will use this cylinder kernel to study the vacuum energy and pressure for several different geometries.

When performing the calculations in this chapter, we use the point-splitting regularization with the point-splitting in the t direction, in order to avoid divergent stress-energy tensor terms. When taking the necessary derivatives, we leave x and x' as separate points. After differentiating, we can set some of these coordinates equal to each other, but we must leave a non-zero separation along one of the coordinates. In this chapter, after taking derivatives, we let $r' = r$, $\theta' = \theta$, and $z = 0$, leaving a nonzero separation only in the t direction, $t' = 0$ and $t \neq 0$. Also, we found that $t^4 T_{\mu\nu}$ (after setting $z = 0$) depends on r and t only in r/t. Because of this, we can simply plot $t = 1$ to observe the behavior for all positive values of t. As the plots show, the energy density and pressures are given as functions of r/t. Where solid curves appear, they give the functions with cutoff still in place. Dashed curves give the behavior when $t = 0$. These curves are calculated by performing a power series expansion of the $T_{\mu\nu}$ components about $t = 0$ and taking the coefficient of the first term. Also, multiple plots within one figure are sometimes plotted with different vertical scales, in order to better show the behavior of the functions.

We now present results computed with Mathematica using the formulas and methods described above. The first, and simplest, case which we consider is that of flat space; then $\theta_1 = 2\pi$. In this case, the cylinder kernel becomes

$$\overline{T} = \frac{1}{4\pi^2 r r'} \frac{1}{\cosh u - \cos\theta}. \tag{2.1}$$

The resulting energy density is $\rho = \frac{3}{2\pi^2 t^4}$, and the pressure components are $p_r = p_\theta = p_z = \frac{1}{2\pi^2 t^4}$. These are independent of the three spatial coordinates, as expected for flat space. As t approaches 0, the components clearly blow up, so we choose to leave a non-zero separation in the t coordinate. Since these quantities are divergent as t approaches the origin, vacuum energy calculations for non-flat spacetimes are often "renormalized"

by subtracting off these divergent terms. We do so for the calculations of energy density and pressure in the Dowker and cone space-times that follow.

The next case we look at is the infinite-sheeted Dowker manifold, where $\theta_1 \to \infty$. Then the cylinder kernel becomes

$$\overline{T}(t,r,\theta,z,r',\theta',z') = -\frac{1}{2\pi^2 rr'\sinh(u)}\frac{u}{u^2+\theta^2}. \tag{2.2}$$

After subtracting the free space term from the energy density and pressure components, we let $r' = r$, $\theta' = \theta$, and $z = 0$. Although we have exact expressions for the components of the stress-energy tensor, the formulas are bulky and cumbersome, so we present the results graphically instead; they are given in figure 1, showing the r/t dependency. All components are independent of the angular coordinate θ. As we move further out into the Dowker space-time, away from the central axis, the energy density and pressure vanish. For T_{pp} and T_{rr}, they diverge as we approach $r \to 0$. Although in the figure they also appear divergent for T_{00} and T_{zz}, taking limits in Mathematica shows that they are in fact finite, with values $1440\pi^2 t^4 T_{00} \to -2160$ and $1440\pi^2 t^4 T_{zz} \to -720$.

We can also take θ_1 to be finite but not equal to 2π as in the case of flat space. The resulting spacetime is then a cone, which is flat space with a wedge of angle $\Delta\theta = 2\pi - \theta_1$ removed. $\overline{T}$ is given by

$$\overline{T} = -\frac{1}{2\pi\theta_1 rr'\sinh(u)}\left(\frac{\sinh(2\pi u/\theta_1)}{\cosh(2\pi u/\theta_1) - \cos(2\pi(\theta-\theta')/\theta_1)}\right). \tag{2.3}$$

It can be recovered from the Dowker space-time by taking an infinite sum over images. The stress-energy tensor components can be calculated here as well, and as mentioned previously, we subtract the divergent free space term. Plots of the components are presented in figure 2 as functions of r/t. All four components remain finite even at $r = 0$.

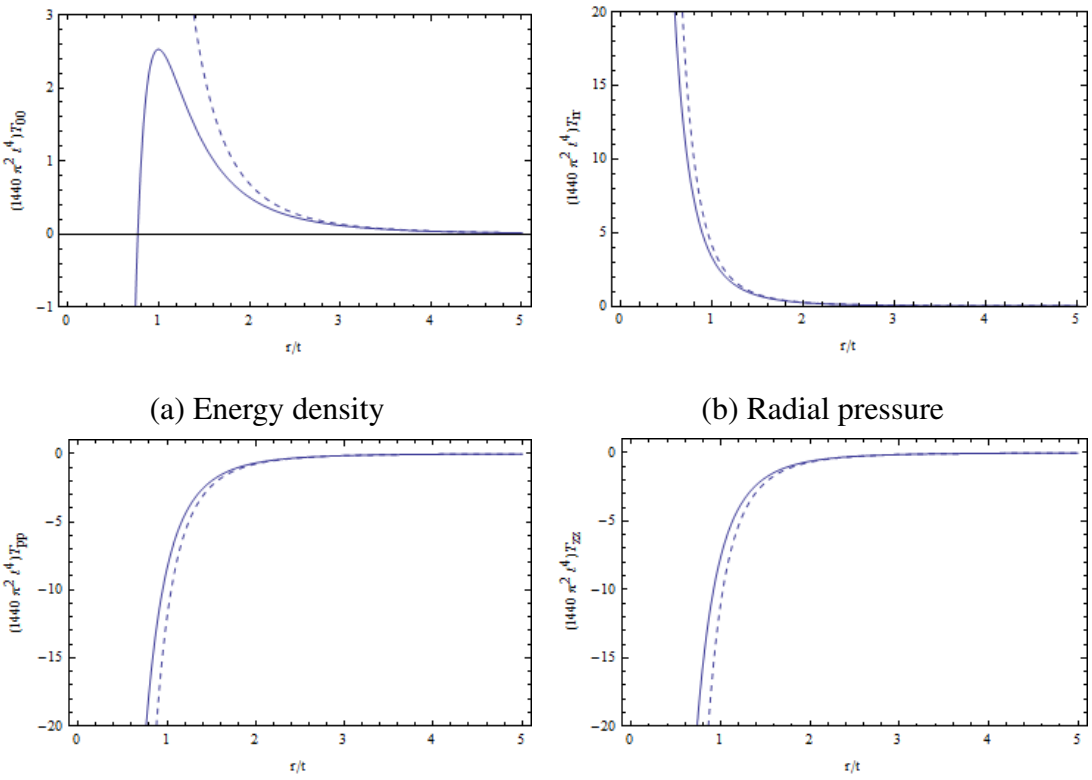

(a) Energy density

(b) Radial pressure

(c) Tangential pressure

(d) Axial pressure

Figure 1. Energy density and pressure as a function of r/t in the Dowker spacetime.

The components have no θ dependency, as one would expect from the symmetry of the situation. In addition to looking at a few specific cases, we can also examine how the $T_{\mu\nu}$ components vary with θ_1. Letting $r = 1$ and $z = 0$ leaves the components as functions of θ_1 only. These are plotted in figure 3. The energy density and pressure components all have a sign change at $\theta_1 = 2\pi$, which is when the cone becomes flat space with a wedge added rather than subtracted. All components are divergent as $\theta_1 \to 0$.

All of these results have been for the case when $\xi = 1/4$ and thus $\beta = 0$. There are, however, additional correction terms to the energy density and pressure components in the case

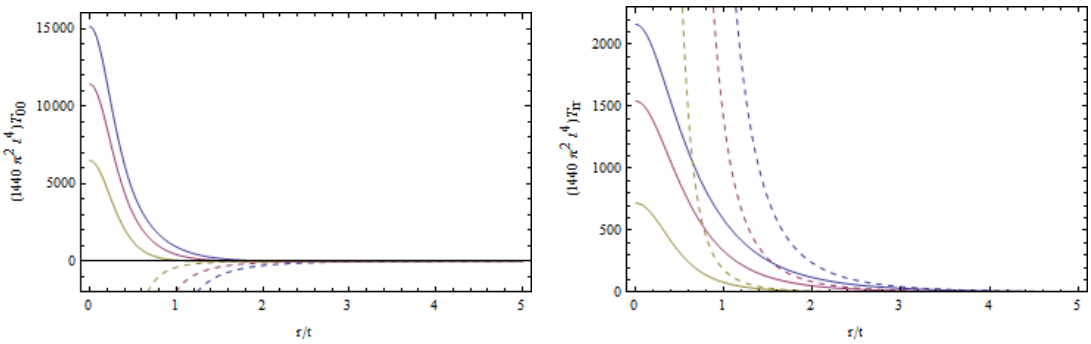

(a) Energy density

(b) Radial pressure

(c) Tangential pressure

(d) Axial pressure

Figure 2. Energy density and pressure as a function of r/t in the cone spacetime, with $\theta_1 = \pi/4$, 1, and $\pi/2$ (blue, red, yellow).

of different values of the coupling parameter which yield a nonzero β. The components given in the following plots are just the additional terms which arise when β is not zero, rather than the whole stress-energy tensor term. For example, $\rho = \beta[\partial_r \partial_{r'} \overline{T} + \partial_r^2 \overline{T} + \frac{1}{r}\partial_r \overline{T}]$ with $\beta = 1$. In the case of flat space, these correction terms are all zero, so no plots are given.

We first revisit the Dowker spacetime. The β terms are given in figure 4. The terms diverge as we approach the central axis.

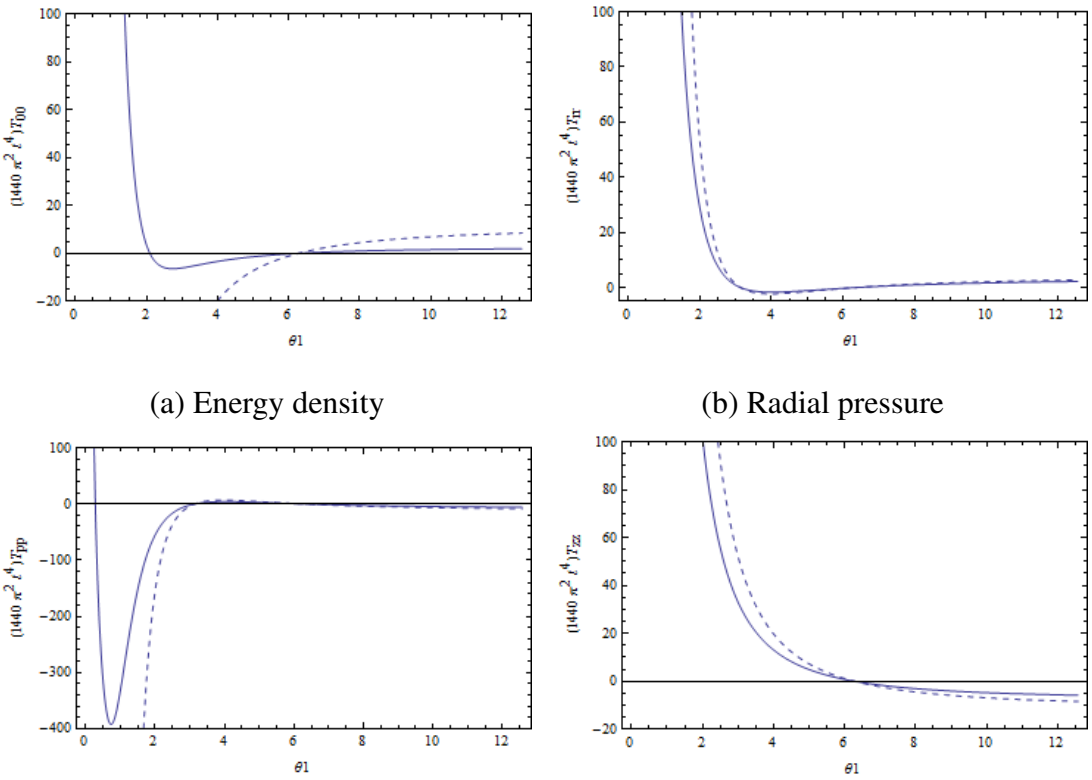

(a) Energy density

(b) Radial pressure

(c) Tangential pressure

(d) Axial pressure

Figure 3. Energy density and pressure as a function of θ_1 in the cone spacetime, with $r = 1$.

For the cone space-time, we look at the correction terms for various values of θ_1. These are plotted in figure 5, as functions of r/t. As in the case of the main part of the stress-energy tensor components given previously in the $\beta = 0$ case, these additional terms are not dependent on θ due to the symmetry of the geometry. They are also finite everywhere.

We conclude this chapter by examining the dependence of the correction terms in the cone geometry on the θ_1 parameter. The results are given in figure 6 for $r = 1$. As with the main part of the stress-energy tensor components, these terms change sign at $\theta_1 = 2\pi$, when the cone has a wedge added rather than subtracted.

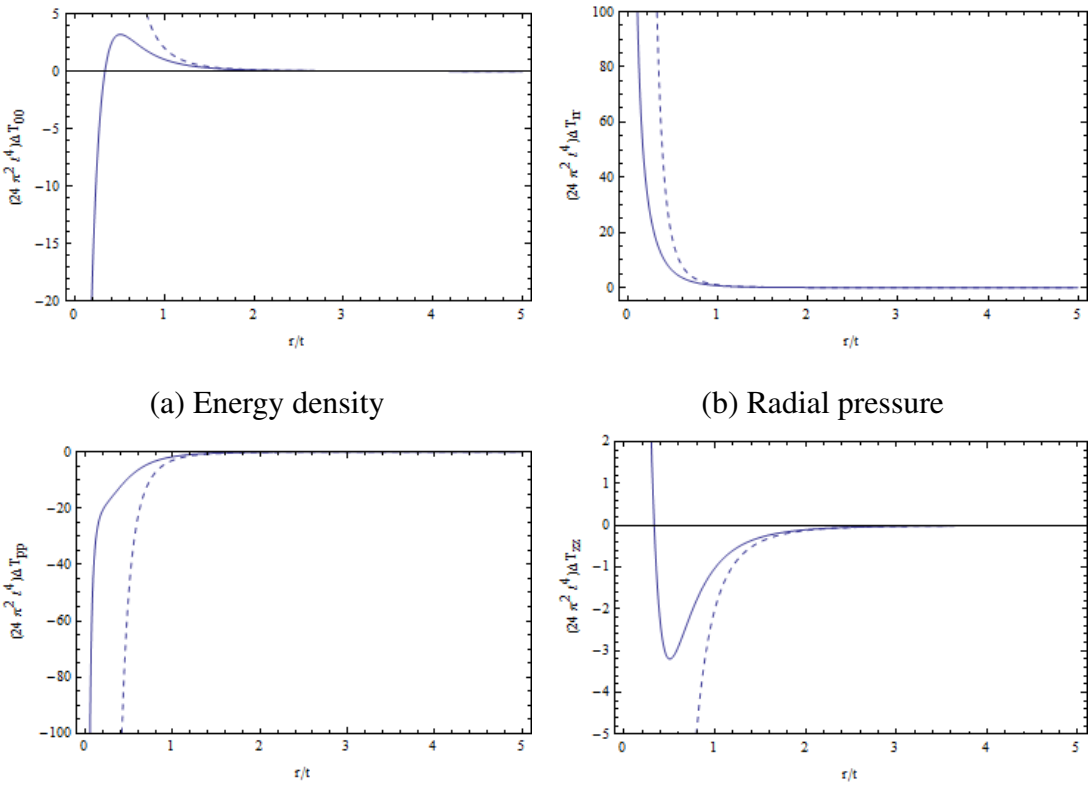

(a) Energy density

(b) Radial pressure

(c) Tangential pressure

(d) Axial pressure

Figure 4. Energy density and pressure correction terms as a function of r/t in the Dowker spacetime, with $\beta = 1$.

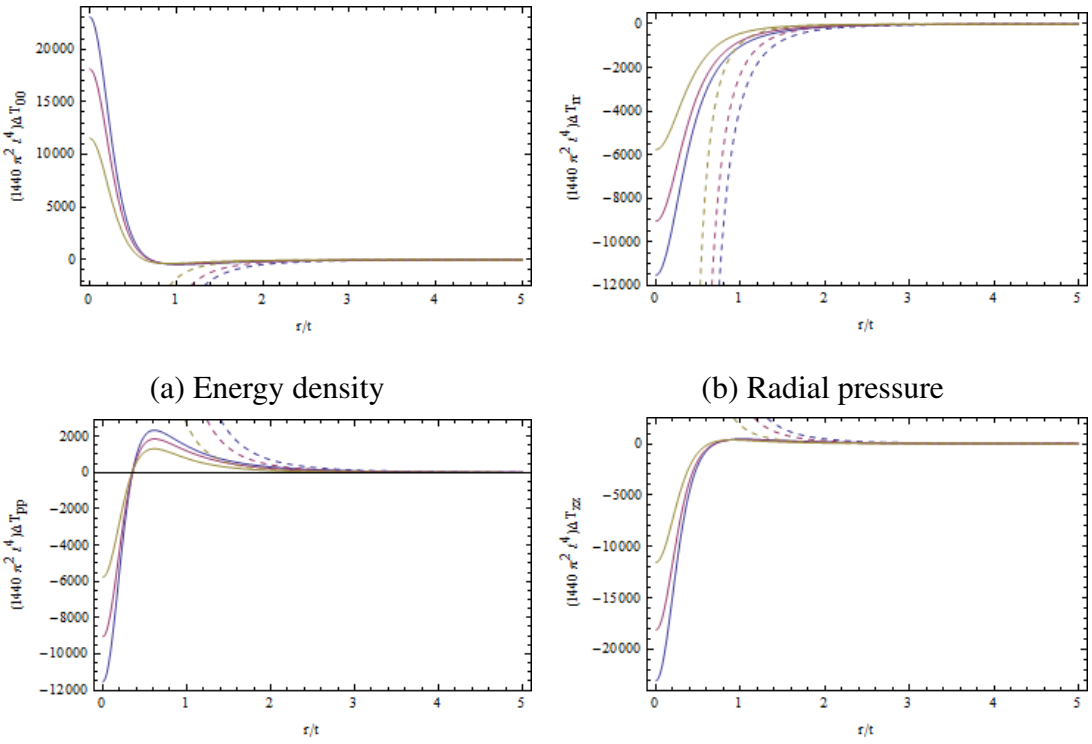

(a) Energy density

(b) Radial pressure

(c) Tangential pressure

(d) Axial pressure

Figure 5. Energy density and pressure correction terms as a function of r/t in the cone spacetime, with $\theta_1 = \pi/4$, 1, and $\pi/2$ (blue, red, yellow).

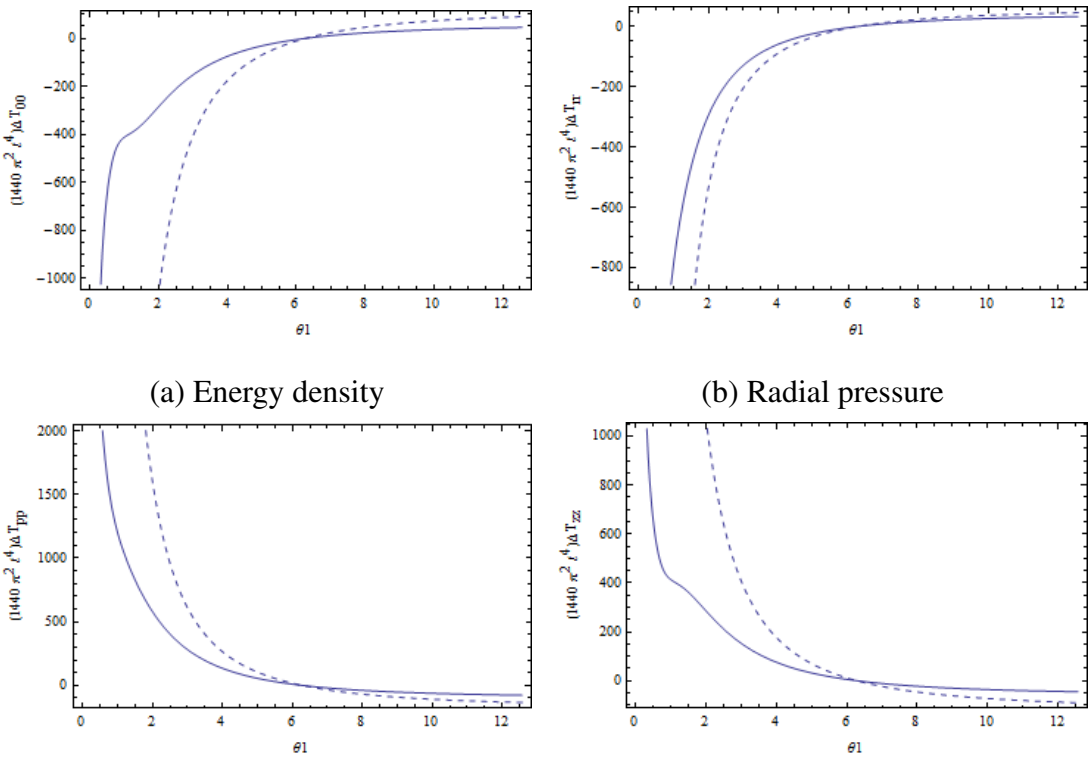

(a) Energy density

(b) Radial pressure

(c) Tangential pressure

(d) Axial pressure

Figure 6. Energy density and pressure correction terms as a function of θ_1 in the cone spacetime, with $r = 1$ (the concavities visible in (a) and (d) are presumably numerical artifacts).

CHAPTER III

WEDGES

We now consider the wedge geometry, consisting of infinite reflecting plates located at $\theta = 0$ and $\theta = \alpha$. In this case, $\overline{T}$ can be constructed by taking an infinite sum over positive and negative images in the infinitely-sheeted Dowker space studied in the previous chapter. The result is

$$\overline{T} = -\frac{1}{4\pi\alpha r r' \sinh(u)} \left(\frac{\sinh(\pi u/\alpha)}{\cosh(\pi u/\alpha) - \cos(\pi(\theta-\theta')/\alpha)} - \frac{\sinh(\pi u/\alpha)}{\cosh(\pi u/\alpha) - \cos(\pi(\theta+\theta')/\alpha)} \right). \tag{3.1}$$

The wedge cylinder kernel can also be constructed by simply taking one image in the cone space-time, with $\theta_1 = 2\alpha$. We use the same expressions for the components of $T_{\mu\nu}$ as we used in chapter 2.

We begin by using the exponential ultraviolet cutoff, as we did for the previous geometries. We let $r = r'$, $\theta = \theta'$, and $z = 0$, with $t \neq 0$. In the calculations that follow, the $T_{\mu\nu}$ components have been renormalized by subtracting the divergent flat-space terms calculated in the previous chapter. Also, as in the previous chapter, dashed curves are for $t = 0$ and solid curves are with the cutoff still in place. Plots are once again given as functions of r/t. We focus only on the wedge of opening angle $\alpha = \pi/2$, but there is no great qualitative difference in the results for other values of α, including those that are not simple rational multiples of π.

When $\beta = 0$, for a wedge of opening angle $\alpha = \pi/2$, results are given in figure 7. This figure gives the energy density and pressures as functions of r/t for various values of θ.

Unlike the case of the cone, the wedge $T_{\mu\nu}$ components depend on θ as well as r. In figure 8, we plot $T_{\mu\nu}$ components as functions of θ for fixed values of r. The functions are symmetric about $\theta = \alpha/2$.

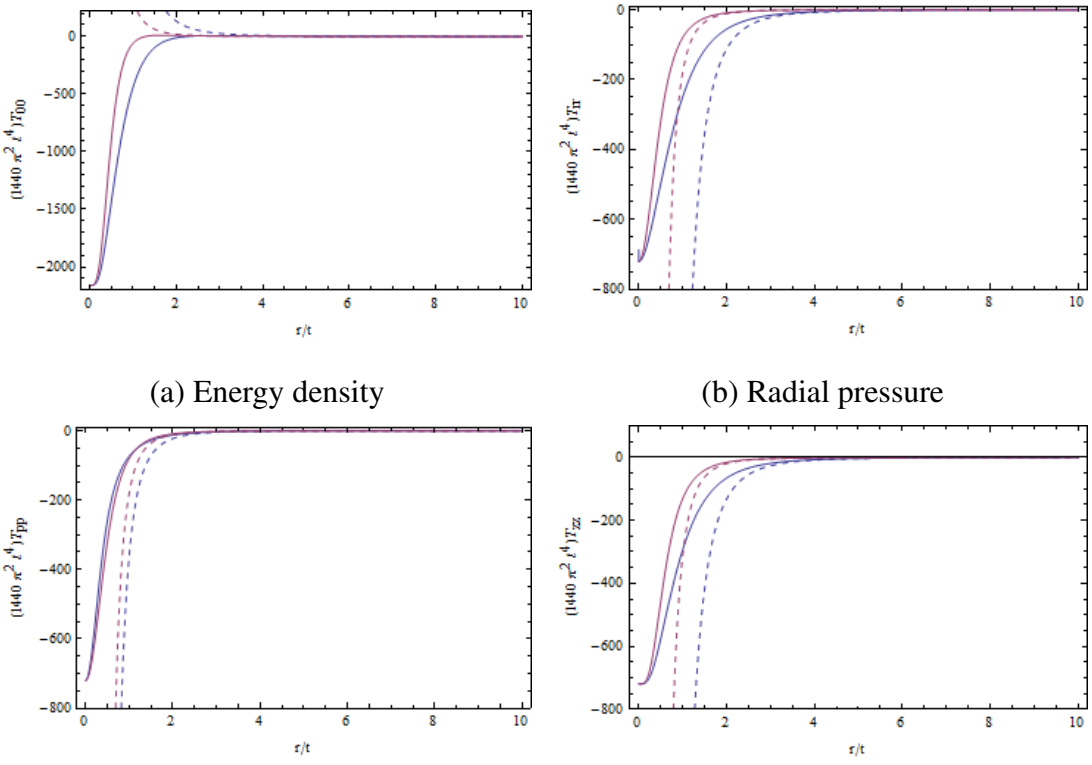

(a) Energy density

(b) Radial pressure

(c) Tangential pressure

(d) Axial pressure

Figure 7. Energy density and pressure as a function of r/t in a wedge of angle $\pi/2$, for $\theta = \pi/8$ (blue) and $\theta = \pi/4$ (red).

We also consider the case when $\beta \neq 0$. Some correction terms are given for the wedge of angle $\alpha = \pi/2$, after letting $\beta = 1$. Figure 9 gives the corrections to $T_{\mu\nu}$ as functions of r/t, while figure 10 presents them as functions of θ.

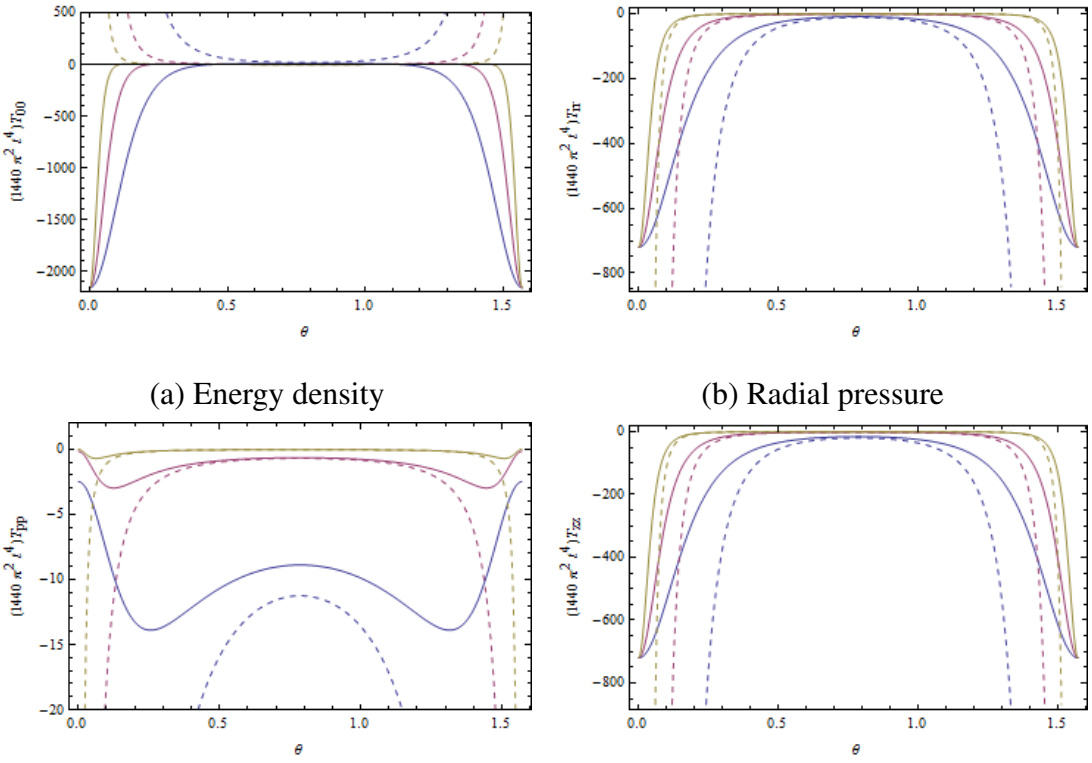

(a) Energy density

(b) Radial pressure

(c) Tangential pressure

(d) Axial pressure

Figure 8. Energy density and pressure as a function of θ in a wedge of angle $\pi/2$, for $r = 2$ (blue), $r = 4$ (red), and $r = 8$ (yellow).

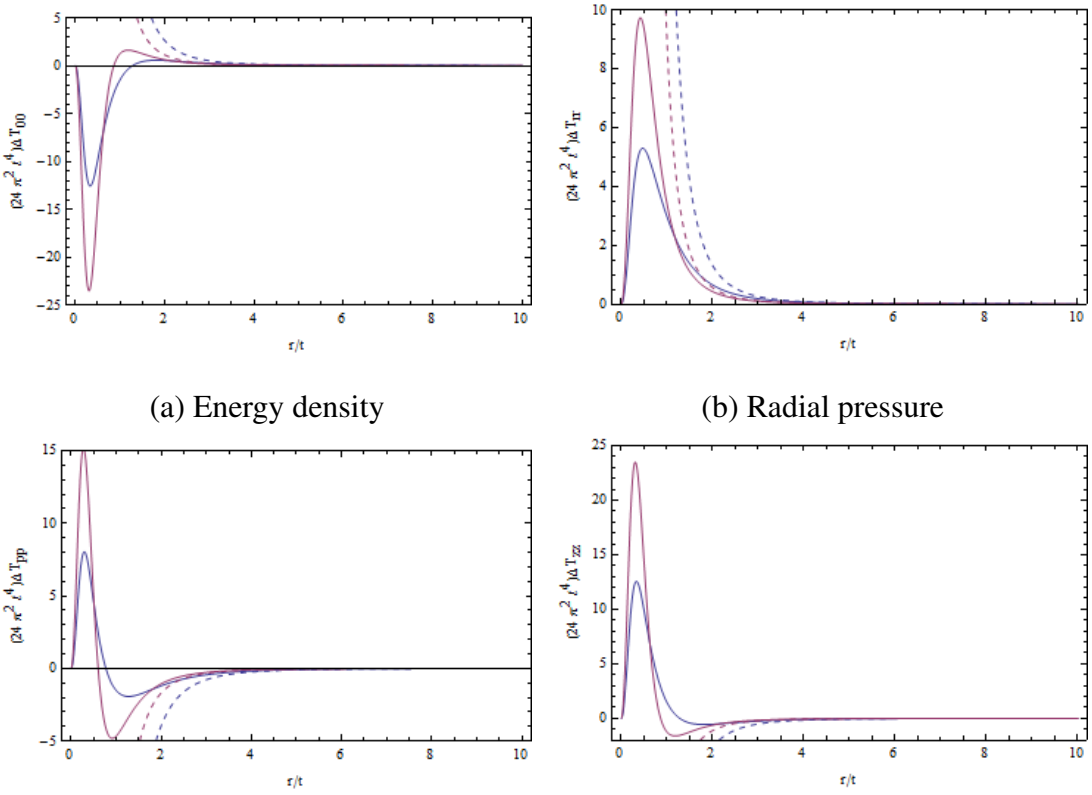

(a) Energy density

(b) Radial pressure

(c) Tangential pressure

(d) Axial pressure

Figure 9. Energy density and pressure corrections as a function of r/t in a wedge of angle $\pi/2$, for $\theta = \pi/8$ (blue) and $\theta = \pi/4$ (red).

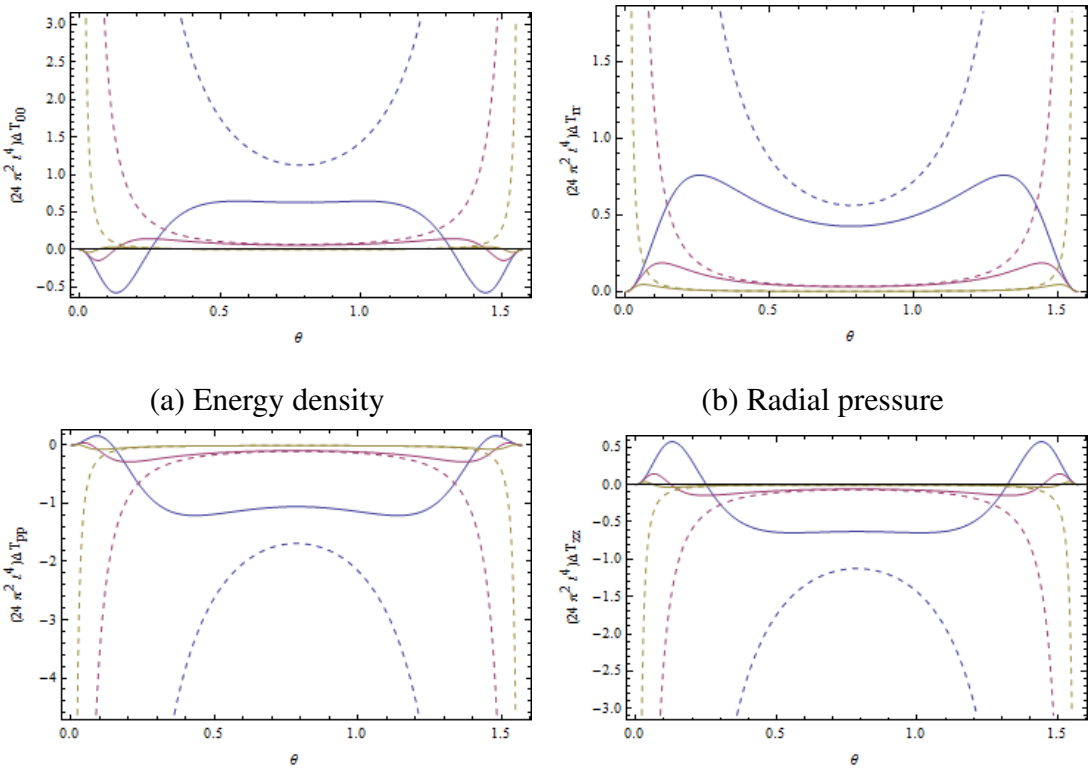

(a) Energy density

(b) Radial pressure

(c) Tangential pressure

(d) Axial pressure

Figure 10. Energy density and pressure corrections as a function of θ in a wedge of angle $\pi/2$, for $r = 2$ (blue), $r = 4$ (red), and $r = 8$ (yellow).

CHAPTER IV

POINT-SPLITTING ALONG Z

As mentioned in the introduction, one current problem with quantum field theory is that in the cutoff case examined in the previous chapters, the energy-balance equation (1.1) is violated. For example, consider the wedge with $\alpha = \pi/2$, and look at the plane at $\theta = \alpha$. One would think that the torque on that plane is balanced by the derivative of the energy density as we change the wedge angle α; in other words, we would expect that

$$\frac{\partial E}{\partial \alpha} = -\int_S r p_p, \tag{4.1}$$

where S is the surface at $\theta = \alpha$ and p_p is the pressure in the direction perpendicular to that plane. However, in the cutoff case studied in chapters 2 and 3, this equation is not satisfied.

We are not restricted to only considering point-splitting in the t direction, however. One may instead perform the point-splitting in a "neutral" direction parallel to the plane, such as the z direction in this case. This method has been used previously in the case of flat space with two reflecting boundaries at $z = 0$ and $x = 0$, with the direction of point-splitting along y [15]. The resulting pressure and energy density were found to satisfy the energy-balance equation. We hoped that applying a similar procedure in the case of cylindrical geometries would also provide results that satisfy the equation. In the case of the wedge with $\alpha = \pi/2$, we have verified that our results for T_{00} and T_{pp} at the reflecting boundaries agree with the corresponding energy density and pressure results for the Cartesian case. However, it currently appears that the torque in the wedge is not canceling; we are not yet confident enough in our calculations to present results here, so examination of this problem will be continued in future work.

In this chapter, we present some preliminary graphical results with the direction of point-splitting along z. We let $r = r'$, $\theta = \theta'$, and $t = 0$, with $z \neq 0$. As was the case with point-splitting along t, we also find that $z^4 T_{\mu\nu}$ depends on r and z only in r/z, so we can plot as functions of r/z. The $T_{\mu\nu}$ components have been renormalized by subtracting the divergent flat-space terms, which are given in this case by $\rho = -\frac{1}{2\pi^2 z^4}$, $p_r = p_\theta = \frac{1}{2\pi^2 z^4}$, and $p_z = -\frac{3}{2\pi^2 z^4}$. Dashed curves are for the no-cutoff case. We also note that because the T_{rr} and $T_{\perp\perp}$ components of $T_{\mu\nu}$ depend on only r and r' derivatives of $\overline{T}$, their values in the cases of point-splitting along t and z are identical. Because of this, we present only plots of T_{00} and T_{zz} in this chapter. Similarly, the plots for the $\beta \neq 0$ correction terms are also unaffected, so we do not repeat them here.

The first geometry we reexamine is that of the Dowker space-time. Results are presented in figure 11, demonstrating the r dependence (for comparison with the results with point-splitting in the t direction, see figure 1). Taking limits reveals that the energy density and axial pressure are finite as $r \to 0$, with values $1440\pi^2 z^4 T_{00} \to 720$ and $1440\pi^2 z^4 T_{zz} \to 2160$. We also examine the cone with finite θ_1. The plots are given in figure 12 for various θ_1 values (compare with figure 2). As we did previously, we can examine how the components of $T_{\mu\nu}$ depend on θ_1, and this dependence is given in figure 13 for $r = 1$ (compare with figure 3).

The next geometry we revisit is the wedge studied in chapter 3. We once again let $\alpha = \pi/2$, and the results are given in figures 14 (compare with figure 7) and 15 (compare with figure 8), as functions of r (for fixed values of θ) and functions of θ (for fixed values of r).

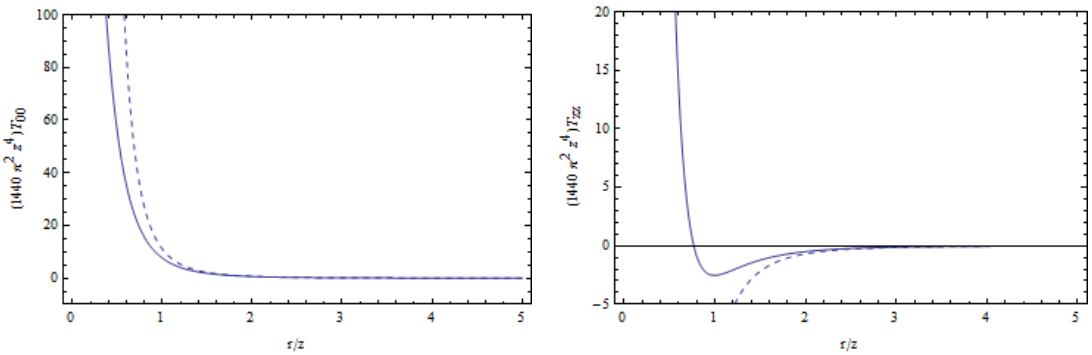

(a) Energy density (b) Axial pressure

Figure 11. Energy density and axial pressure as a function of r/z in the Dowker spacetime.

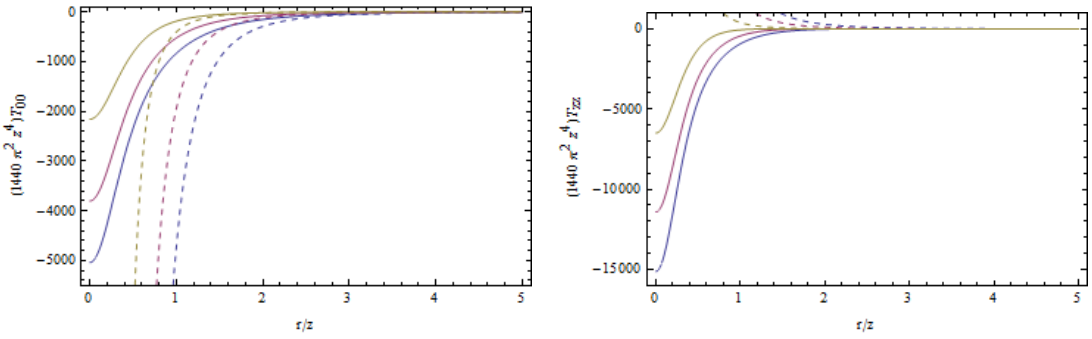

(a) Energy density (b) Axial pressure

Figure 12. Energy density and axial pressure as a function of r/z in the cone spacetime, with $\theta_1 = \pi/4$, 1, and $\pi/2$ (blue, red, yellow).

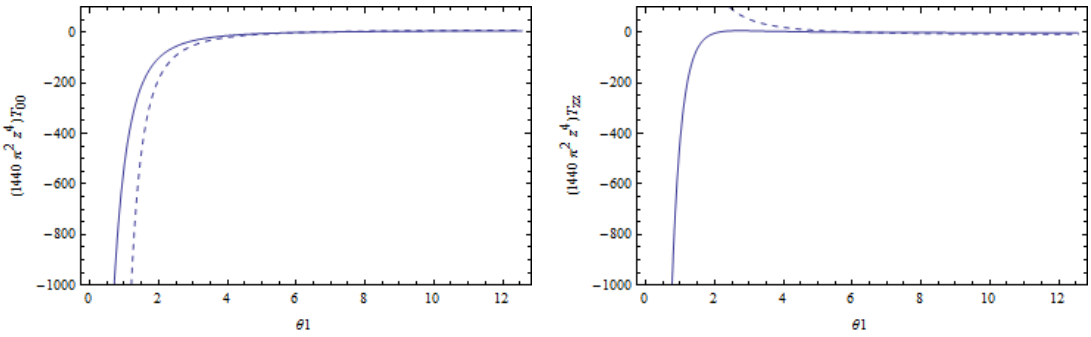

(a) Energy density (b) Axial pressure

Figure 13. Energy density and axial pressure as a function of θ_1 in the cone spacetime, with $r = 1$.

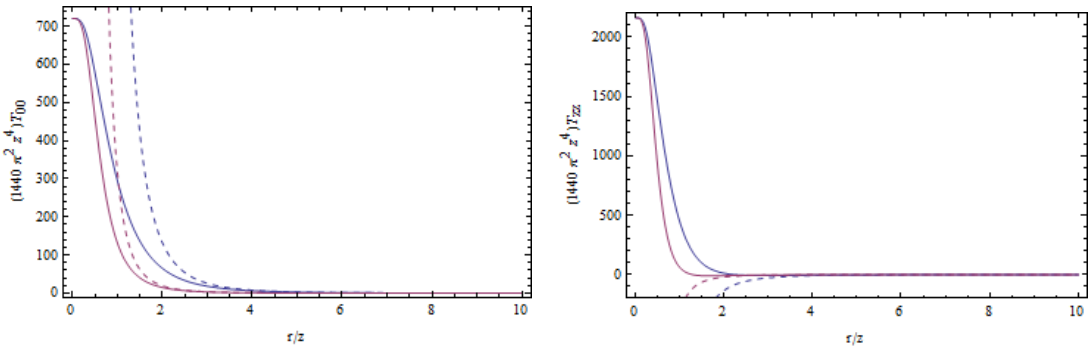

(a) Energy density (b) Axial pressure

Figure 14. Energy density and axial pressure as a function of r/z in a wedge of angle $\pi/2$, for $\theta = \pi/8$ (blue) and $\theta = \pi/4$ (red).

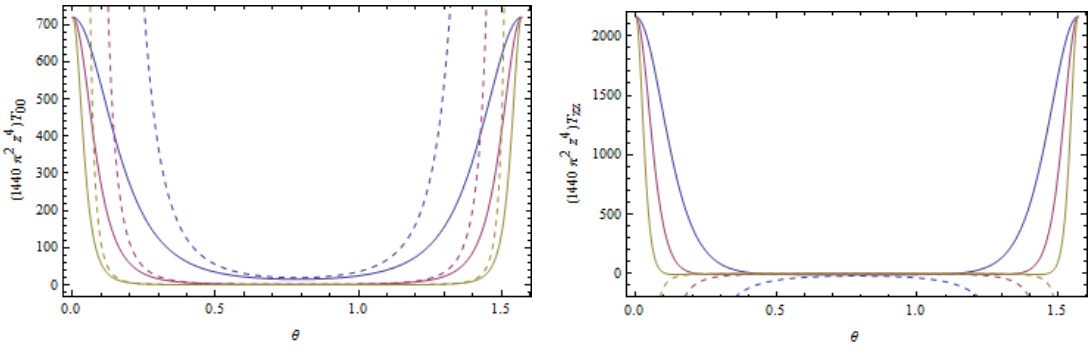

(a) Energy density (b) Axial pressure

Figure 15. Energy density and axial pressure as a function of θ in a wedge of angle $\pi/2$, for $r = 2$ (blue), $r = 4$ (red), and $r = 8$ (yellow).

CHAPTER V

CONCLUSION

We have successfully calculated the vacuum energy density and pressure for various cylindrically symmetric systems (flat space, the infinitely sheeted Sommerfeld-Dowker manifold, cones of finite angle, and an infinite wedge). Calculations were initially performed using point-splitting in the t direction, and plotted in comparison to the results with no cutoff in place. When using this cutoff, however, the energy-balance equation is often violated. Things may be rectified if one performs the point-splitting in a neutral direction; this has been done for the case of two intersecting planes in Cartesian coordinates, and the energy balance equation was satisfied there. Some preliminary calculations have been presented here using point-splitting in the z direction, but further analysis is required to determine if the energy-balance equation is satisfied here as well. Future work may focus on such calculations, in order to help us understand this particular issue.

REFERENCES

[1] Fulling S A 1989 *Aspects of Quantum Field Theory in Curved Space-Time* (Cambridge, UK: Cambridge University Press)

[2] Fulling S A 2010 *Internat. J. Mod. Phys.* **25** 2364

[3] Schwartz-Perlov D and Olum K D 2005 *Phys. Rev. D* **72** 065013

[4] Liu Z H 2009 *Closed Path Approach to Casimir Effect in Rectangular Cavities and Pistons*, Ph.D. dissertation (Texas A&M University, College Station) http://www.math.tamu.edu/ fulling/qvac09/liudiss.pdf

[5] Lukosz W 1973 *Z. Physik* **262** 327

[6] Dowker J S 1977 *J. Phys. A* **10** 115

[7] Dowker J S 1987 *Phys. Rev. D* **36** 3095

[8] Futamase T and Garfinkle D 1988 *Phys. Rev. D* **37** 2086

[9] Smith A G 1990 Gravitational effects of an infinite straight cosmic string on classical and quantum fields: Self-forces and vacuum fluctuations in *The Formation and Evolution of Cosmic Strings* ed. G Gibbons S Hawking and T Vachaspati (Cambridge, UK: Cambridge University Press) pp 263-292

[10] Truong M 2008 Vacuum Energy in Wedges and Around Cosmic Strings, Unpublished Manuscript (Texas A&M University) http://www.math.tamu.edu/˜stephen.fulling/qvac08/truong/

[11] Dowker J S 1978 *Phys. Rev. D* **18** 1856

[12] Linet B 1987 *Phys. Rev. D* **35** 536

[13] Trendafilova C 2011 *Static, Cylindrical Symmetry in General Relativity and Vacuum Energy*, Undergraduate Research Scholars thesis (Texas A&M University, College Station)

[14] Fulling S A, Kaplan L, Kirsten K, Liu Z H and Milton K A 2009 *J. Phys. A: Math. Theor.* **42** 155402

[15] Fulling S A, Milton K A and Wagner J 2012 Energy density and pressure in power-wall models *Internat. J. Mod. Phys. Conf. Ser.* in press

APPENDIX A

MATHEMATICA FILES

We include three supplementary files in the form of Mathematica notebooks. These provide examples demonstrating the procedure used for calculations in this thesis. The first file, "AppendixA1.nb", includes calculations for flat space with point-splitting in the t direction. The second file, "AppendixA2.nb", shows various calculations for the cone space with point-splitting once again in the t direction. The final file, "AppendixA3.nb", contains calculations for the wedge with point-splitting in the z direction.

CONTACT INFORMATION

Name:	Cynthia Trendafilova
Professional Address:	c/o Dr. Stephen Fulling Department of Mathematics MS 3368 Texas A&M University College Station, TX 77843
Email Address:	cyntrendafilova@gmail.com
Education:	B.S., Physics, Texas A&M University, May 2012 B.S., Mathematics, Texas A&M University, May 2012 Undergraduate Research Scholar Honors Research Fellow Phi Beta Kappa Pi Mu Epsilon Sigma Xi